

See discussions, stats, and author profiles for this publication at: <https://www.researchgate.net/publication/215451132>

# Effect of Halide Ion Adsorption upon Plasmon-Mediated Photoelectron Emission at the Silver/Solution Interface

ARTICLE *in* THE JOURNAL OF PHYSICAL CHEMISTRY B · JUNE 1997

Impact Factor: 3.3 · DOI: 10.1021/jp9640080

CITATIONS

25

READS

21

## 3 AUTHORS:



**Milan Fedurco**

Michelin Switzerland

54 PUBLICATIONS 2,871 CITATIONS

SEE PROFILE



**Valery Shklover**

ETH Zurich

7 PUBLICATIONS 257 CITATIONS

SEE PROFILE



**Jan Augustynski**

University of Geneva

111 PUBLICATIONS 3,939 CITATIONS

SEE PROFILE

## Effect of Halide Ion Adsorption upon Plasmon-Mediated Photoelectron Emission at the Silver/Solution Interface

M. Fedurco,<sup>†</sup> V. Shklover,<sup>‡</sup> and J. Augustynski<sup>\*,†</sup>

Département de Chimie Minérale, Analytique et Appliquée, Université de Genève,  
CH 1211 Genève 4, Switzerland, and Laboratorium für Kristallographie,  
ETH Zentrum, CH-8092 Zürich, Switzerland

Received: December 6, 1996<sup>®</sup>

The effect of the roughening of the silver surface upon photoemission observed in the presence of two different scavengers dissolved in an aqueous solution, CO<sub>2</sub> and NO<sub>3</sub><sup>−</sup> ions, was re-examined. The quantum yield of the photocurrent exhibits a sharp maximum at 370–380 nm in the frequency range of surface plasmons on silver. These photoyields were strongly affected by the extent of the roughening of the Ag surface and reached an unusually large value of 0.05 electron per incident photon. Electrochemical oxidation/reduction roughening performed in the presence of Cl<sup>−</sup>, Br<sup>−</sup>, and ClO<sub>4</sub><sup>−</sup> ions, similar to that employed in enhanced Raman scattering (SERS) experiments, affected the maximum of the photocurrent and in some cases also its onset potential. Photocurrents arising at potentials more negative than the potential of zero charge (pzc) of silver were principally influenced by changing morphology of the surface resulting from more or less deep roughening performed in different solutions. On the other hand, the photoelectrochemical behavior of silver at potentials positive with respect to the pzc was clearly affected by the specific adsorption of anions of the supporting electrolyte. It was, in particular, the Br<sup>−</sup> anion that caused in this potential region the strongest enhancement of the photocurrent, associated with the reduction of scavengers and led to an apparent positive shift of the onset potential. The role played by the specifically adsorbed anions is interpreted in terms of slowing down the reverse reactions of solvated electrons and of reaction intermediates (such as, for example, the NO<sub>3</sub><sup>2−</sup> anion) returning to the electrode.

### Introduction

A number of phenomena, such as surface-enhanced Raman scattering (SERS),<sup>1</sup> photodissociation of organic molecules,<sup>2</sup> or photoemission of electrons at the Ag/vacuum<sup>3</sup> and Ag/solution<sup>4</sup> interfaces, were found to depend strongly on the morphology of the silver metal surface. Procedures for the preparation of microscopically rough silver surfaces used in such studies involved chemical etching, electrochemical roughening, mechanical polishing of Ag with varying size of alumina, and metal sputtering in vacuum on various pre-etched substrates. Dawson et al.<sup>5</sup> used the latter approach, depositing thin films of silver on glass-roughened CaF<sub>2</sub> or NaCl substrates. The size of Ag particles was found in this case to depend markedly on the rate of film deposition. Slowly deposited silver films consisted typically of particles of about 150 nm diameter and yielded much more intense SERS signals for adsorbed benzoic acid (Kretschmann configuration, incident laser light of 647.1 nm) compared to fast deposited Ag films with approximately 40 nm particle diameter. Tuschel et al.,<sup>6</sup> who prepared the silver surface by electrochemical oxidation/reduction roughening in 1 M NaCl, found on average a nodule size of ca. 100 nm (with the features ranging from 40 to 180 nm) to cause the strongest enhancement of the SERS signal due to adsorbed Cl<sup>−</sup> ions. Importantly, these authors, employing a double-potential step sequence, noted that the average diameter of formed nodules, interfeature distance, and nodule surface concentration are controlled principally by the rate of oxidation of silver and are practically independent of the subsequent silver chloride reduction rates. The size of the surface features produced on silver

by such a method has been shown to decrease with increasing the oxidation rate.

In photoemission into solution experiments, the observed increase in photocurrent upon roughening of the Ag surface is less dramatic than the corresponding enhancement of the optical signal observed in SERS. However, a 10–100-fold increase in the values of photocurrent upon electrode surface roughening is not uncommon in such studies.<sup>4c,7</sup> For example, the quantum yield per incident photon for carbon dioxide photoreduction on electrochemically roughened Ag has been shown to increase about 10 times at 380 nm and ca. 30 times at 514 nm with respect to a nominally smooth surface.<sup>4c</sup> In the latter study, the electrochemical roughening of the Ag surface was performed in perchlorate solutions by cycling the electrode potential, at 1 V/s, between −1.0 and 0.9 V vs Hg/HgO/0.1 M NaOH reference electrode (several hundred cycles). However, such a procedure results in a quite heterogeneous distribution of the roughness features.

The first purpose of the present work was to establish if there exists a correlation between the size (i.e., the height and the diameter) and distribution of the Ag surface features, on one hand, and the amount of the photoemission current determined in the solutions containing dissolved CO<sub>2</sub> or NO<sub>3</sub><sup>−</sup> ions acting as scavengers, on the other. In order to prepare Ag surfaces with controlled morphologies, we adopted the double-potential step procedure closely similar to that described in ref 6. This opened an additional possibility to compare the effect of Ag surface morphology on the photoemission currents, with the corresponding effect on the intensity of the SERS signals observed by the above mentioned authors.<sup>6</sup> The comparison was further extended to silver electrodes roughened and consecutively submitted to photoemission experiment in the solutions containing bromide ions. In contrast with the ClO<sub>4</sub><sup>−</sup>

<sup>†</sup> Université de Genève.

<sup>‡</sup> ETH Zentrum.

<sup>®</sup> Abstract published in *Advance ACS Abstracts*, June 1, 1997.

anion, which is only weakly adsorbed on silver, the  $\text{Br}^-$  and  $\text{Cl}^-$  anions are specifically adsorbed, and therefore, the question arises whether they affect directly the process of photoemission at silver.

### Experimental Section

Electrochemical experiments were performed in a two-compartment cell equipped with a quartz window. A platinum counter electrode (large area Pt grid) was separated from a silver working electrode by a Nafion membrane. A Ag rod of 0.55 or 0.7 cm i.d. (Specpure 99.999%, Johnson Matthey) embedded in a Teflon cylinder served as the working electrode. The electrode surface was prepared by polishing mechanically the Ag rod with fine emery papers and then with suspensions of 1.0 and 0.3  $\mu\text{m}$  alumina powders on a polishing Mecaprex disk (Well). Alumina was removed from the electrode surface via sonication in an ultrasonic bath and washing with a copious amount of distilled water. Before photoelectrochemical measurements, possible traces of oxide were removed from the electrode surface by cycling the potential into the hydrogen evolution region<sup>8</sup> (three voltammetric scans from  $-0.2$  to  $-1.8$  V and back in aqueous perchlorate solution). All potentials were measured against a Hg/HgO/1.0 M NaOH reference electrode (0.09 V negative vs the saturated calomel electrode). Roughened silver surfaces were examined at 30 kV accelerating voltage in a Hitachi S-900 "in-lens" field-emission scanning electron microscope. Photoelectrochemical experiments were carried out using a chopped light from a Spectra Physics Model 2025-04 argon-ion laser (334.0, 351.1, and 363.8 nm emission lines). The absolute intensity of the incident light was measured with a laser power/energy meter (Model DG, Newport Instruments). The light was modulated mechanically either using a chopper at a frequency of 7.2 Hz or by means of an electric shutter at 300 or 500 ms intervals. The photocurrent was recorded at a normal incidence of light on the vertically mounted electrode, using a Stanford Research Systems lock-in amplifier type SR 530. Some experiments were performed using light from a Multispec 257 monochromator (Oriol). The electrochemical equipment consisted of an Elpan potentiostat and an Elpan waveform generator controlled by a dedicated micro-computer employing Keithley DAS 20 hardware. Gaseous reaction products were analyzed on a Hewlett Packard 5890 Series II gas chromatograph equipped with a FID and a TCD detector.

All solutions were freshly made from reagent grade chemicals and twice distilled water. The measurements were performed at room temperature,  $22 \pm 1$  °C.

### Results and Discussion

As shown in Figure 1, roughening of silver in the solutions containing chloride and bromide ions results in markedly different surface morphologies. Figure 1a–d represent typical scanning electron microscopy (SEM) images of the Ag surface roughened in 1.0 M NaCl. In this case, the roughening was performed by stepping the electrode potential from the open circuit value to  $+0.2$  V located in the Ag oxidation region, where the anodic current density reached about  $7 \text{ mA cm}^{-2}$ , and then back to  $-0.2$  V, where the silver halide undergoes reduction. The Ag surface roughened in such a way (Figure 1a,b) consists of almost spherical nodules, about 100 nm in diameter, fused together during the nucleation process. Since the depth parameter of the roughened surface was not determined by the previous authors,<sup>6</sup> we have attempted to fracture the Ag samples in order to estimate the height of the nodules. Figure 1d shows that, on average, the nodules, including those fused together,

have a height of about 100 nm. Note that present on the relatively smooth areas without large nodules, perceptible in Figure 1c, are small hemispherical nucleation centers, about 10–20 nm in diameter, emerging from the underlying substrate (Figure 1d).

Parts e–g of Figure 1 represent a top view and Figure 1h shows a cross sectional view of the Ag samples roughened in a 1.0 M NaBr solution. Like in the former case, the double-potential step method was used, and both the oxidation current density and the total anodic charge were similar to those adopted during the Ag roughening in 1 M NaCl. This surface consists of a network of three-dimensionally grown clusters. As a rule, the electrode surfaces prepared through the oxidation/reduction sequence in bromide solutions appeared to be significantly more branched than those obtained in the presence of chlorides. This probably reflects the superior ability of bromides to complex  $\text{Ag}^+$  ions during the silver dissolution process as well as a different kinetics of AgBr reduction compared to that of  $\text{AgCl}$ .<sup>9,10</sup> As shown in Figure 1h, the height of metallic clusters at the silver roughened in bromide solution may reach 800 nm.

Despite an apparently larger extent of roughness, the silver electrode pretreated, according to the above description, in 1 M NaBr solution yielded about 2 times lower photocurrents for  $\text{CO}_2$  reduction than that roughened in 1 M NaCl (cf. Figure 2). However, it is to be recalled that surface roughness can induce effective coupling of light to surface plasmons, only providing that it has the correct spatial Fourier components to conserve both wavevector and energy in the process. Any extra random roughness to the small amplitude sinusoidal grating will cause damping of the excited surface plasmons, broadening of the narrow resonance, and intensity loss in the local surface field.<sup>11</sup> Theoretical calculations pertaining to the enhancement of local electric field due to excitation of surface plasmons point at the shape of roughness features as being an important parameter.<sup>12</sup> Thus, the highest average enhancement is predicted for oblate spheroids.<sup>12</sup> The aspect of the Ag surface formed in 1 M NaCl is evidently much more close to such a description than that of the surface being roughened in 1 M NaBr (Figure 1). In particular, the former is characterized by the average ratio of nodule height to diameter close to 1, while for the latter surface the corresponding ratio is much larger, reaching 8 for several features.

In order to establish a more detailed relationship between the surface morphology of silver and the amount of photoemission currents, a series of electrochemical double-potential step pretreatments were carried out in 1 M NaCl solution. The choice of the latter solution was dictated by the possibility of creating a relatively uniform morphology and to change, within certain limits, the size of nodules while avoiding to a large extent a three-dimensional growth.<sup>6</sup> To verify the kind of dependence of the photocurrent on the surface concentration of nodules, the silver electrode has been oxidized at increasing potentials of 0.15, 0.175, 0.2, 0.25, and 0.35 V, respectively, to reach a constant total anodic charge equal to  $20 \text{ mC cm}^{-2}$ . At lower potentials and smaller current densities (e.g.,  $3.5 \text{ mA cm}^{-2}$ ) the Ag oxidation in 1.0 M NaCl has been reported to create about 10 nodules/ $\mu\text{m}^2$ , while for a large anodic current of  $18 \text{ mA cm}^{-2}$  the average number of nodules increased to 54 per  $\mu\text{m}^2$ .<sup>6</sup> The increase in the concentration of nodules, due to their smaller size, was accompanied by an increase in the interfeature distance. According to the above report,<sup>6</sup> there is a significant enhancement in the SERS signal corresponding to a  $\nu(\text{Ag}-\text{Cl})$  vibration at  $235 \text{ cm}^{-1}$  as a result of the silver roughening at anodic current densities approaching  $20 \text{ mA cm}^{-2}$ . Under such conditions, an average nodule diameter is about 100 nm. We

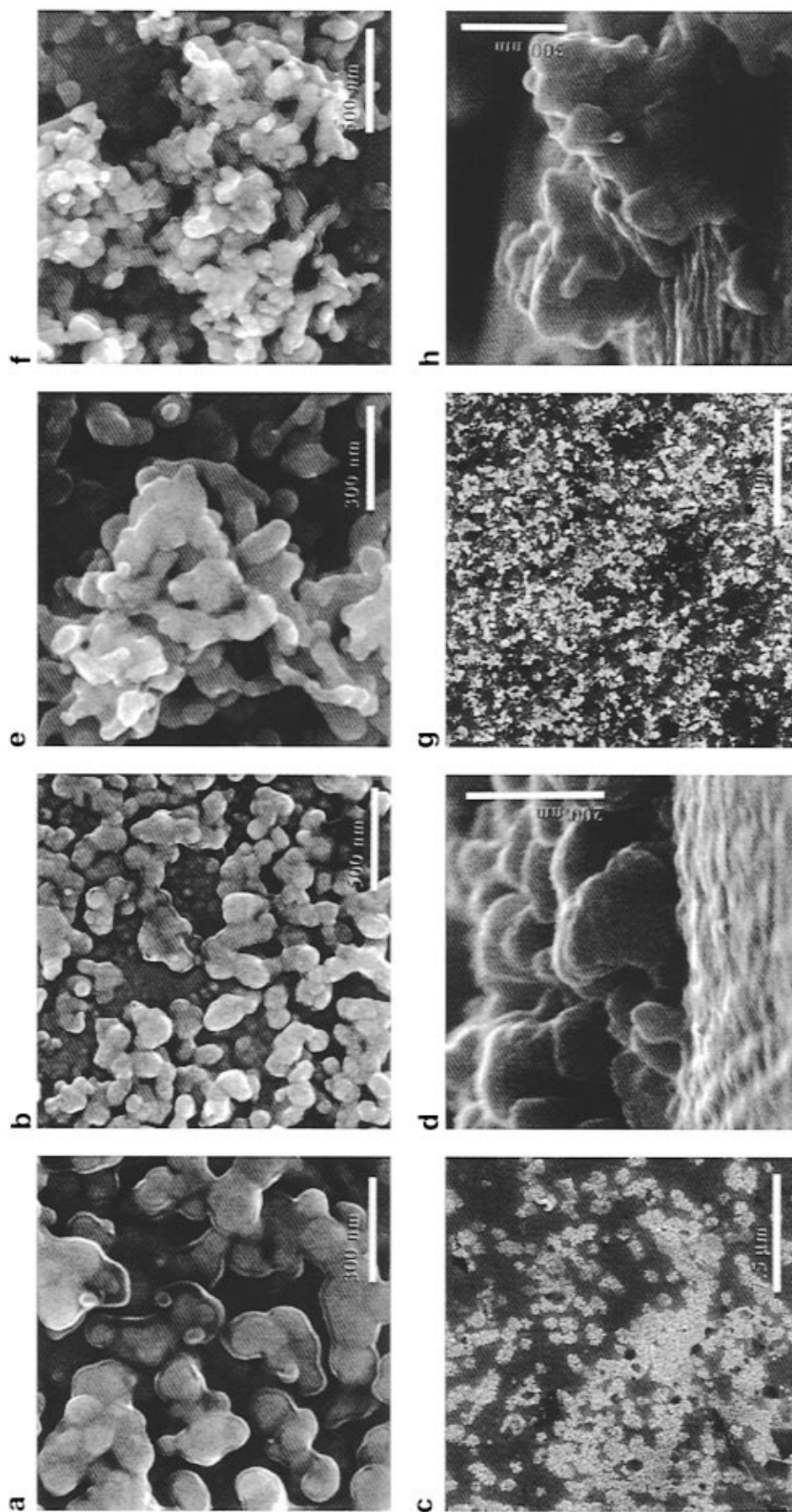


**Figure 1.** Scanning electron microscopy images of Ag surfaces roughened electrochemically in 1.0 M NaCl at +0.20 V (oxidation current density was 7 mA cm<sup>-2</sup>, 20 mC cm<sup>-2</sup> passed), AgCl reduction at -0.20 V (a-d), and in 1.0 M NaBr at +0.030 V (oxidation current density 9 mA cm<sup>-2</sup>, 20 mC cm<sup>-2</sup> passed), AgBr reduction at -0.23 V (e-h). Micrographs d and h show cross sectional view of the samples.

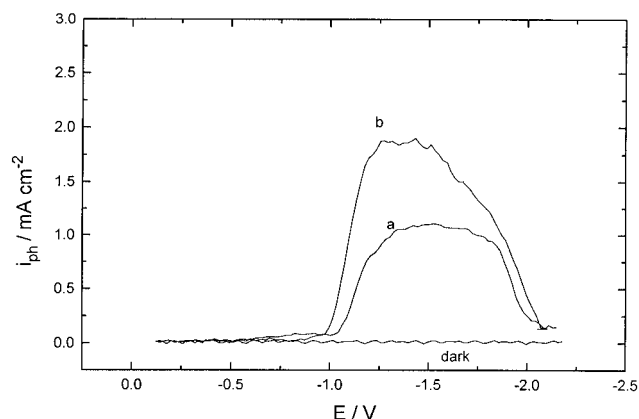


**Figure 2.** Dependence of the cathodic photocurrent on electrode potential for the reduction of  $\text{CO}_2$  to  $\text{CO}$  recorded on silver electrodes roughened electrochemically as described in Figure 1. The electrode was illuminated with a 400 mW argon laser beam (334, 351.1, and 363.8 nm lines) and polarized cathodically at a scan rate of 100 mV/s (chopped light at 7.0 Hz). Saturated  $\text{CO}_2$  solution. Roughening performed in 1.0 M NaBr (a) and 1.0 M NaCl (b).

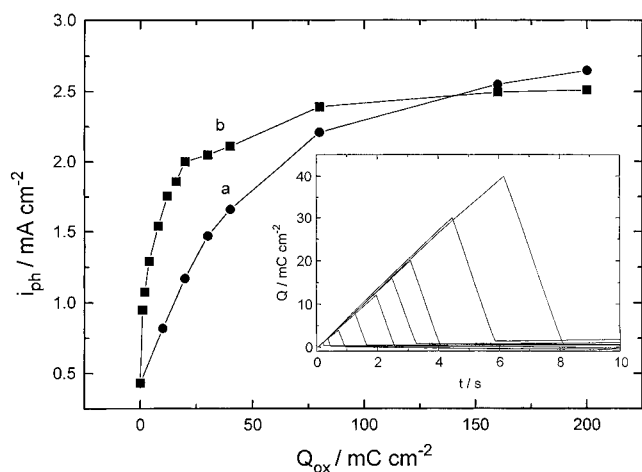


**Figure 3.** Photocurrent due to the reduction of  $\text{CO}_2$  to  $\text{CO}$  at  $-1.2$  V plotted as a function of anodic charge density ( $Q_{\text{ox}}$ ) passed during the silver oxidation in 1.0 M NaBr at 0.03 V (a) and for Ag roughened in 1.0 M NaCl at 0.20 V (b). Inset shows typical  $Q_{\text{ox}}-t$  plots for symmetrical potential jump experiments with varying amounts of charge passed during the Ag oxidation at  $+0.20$  V and AgCl reduction at  $-0.20$  V, respectively.

found that a similar increase in the silver oxidation current density, up to  $30 \text{ mA cm}^{-2}$ , results in a sizable, about 25%, increase of the photocurrent for  $\text{CO}_2$  reduction at  $-1.2$  V (1.0 M NaCl).

Bryant and Pemberton<sup>13</sup> examined silver samples, roughened in 0.1 M KCl solution using the double-potential step method, by means of differential reflectance spectroscopy. The largest decrease in reflectivity occurred for the surfaces preoxidized at higher current densities and, thus, composed of the smallest nodules (100–300 nm in size). The observed relationship between reflectivity and the size of the roughness features was assigned to changes in light absorption by such roughened Ag surfaces.<sup>13</sup> This is certainly one of the reasons for the changes in cathodic photocurrents as a function of the conditions of electrochemical roughening noted in our experiments.

Interestingly, deeper roughening of the Ag surface causes further increase of the photocurrent. This is illustrated by the photocurrent vs anodic charge curves shown in Figure 3 for silver electrodes pretreated in 1 M NaCl compared to 1 M NaBr solution. The anodic charge refers here to the total charge passed during a single oxidation step employed to roughen the

Ag surface. The inset in Figure 3 shows the dependence of the amount of charge on time for the oxidation of silver in 1.0 M NaCl at  $+0.2$  V, followed by the reduction at  $-0.2$  V. As seen from these  $Q-t$  plots, the rates of Ag oxidation and those of AgCl reduction are approximately constant and independent of the amount of charge passed during both processes. As shown in Figure 3, a relatively mild roughening in 1 M NaCl produces a sharp increase of the photocurrent, which finally levels off for the oxidation charge exceeding  $100 \text{ mC cm}^{-2}$ . On the other hand, Ag electrodes roughened in 1 M NaBr exhibited a progressive rise of the photocurrent with increasing the oxidation charge up to  $200 \text{ mC cm}^{-2}$ . Importantly, a deep roughening of the Ag surface (corresponding to the passage of  $200 \text{ mC cm}^{-2}$ ) in both solutions produces quite comparable results with regard to the amount of the measured photocurrent (cf. Figure 3). Roughening of silver at a still more positive potential of  $+0.5$  V resulted in about 50% decrease of cathodic photocurrents despite an apparent increase in the surface area. Under such conditions, the electrode surface may remain partly blocked by unreduced insulating AgCl or AgBr layers inhibiting the electron transfer.

The value of the electrode potential at which the photoelectrochemical measurements reported in Figure 3 were carried out ( $-1.2$  V) allows the assignment of the observed variation of the photocurrent solely to the morphological changes of the silver surfaces. In fact, at such a negative potential the coverage of the chloride and bromide species adsorbed on silver may be considered as negligible.<sup>14</sup> When considering the correlation between the extent of surface roughness and the amount of plasmon-mediated photoemission currents, it is worthy of recalling that an optically excited plasmon may cause the photoemission only if it decays into a single-particle (one-electron) excitation, leading to a final state electron with energy exceeding the work function.<sup>15</sup> The striking feature of such a process, first noted in the case of photoemission measurements at an Al/vacuum interface,<sup>15</sup> was a strong enhancement of the photoyield associated with roughening of the surface, exceeding by far the corresponding reflectance change on the same surface. In this connection, the enhancement of electromagnetic field density at the interface appears as a more important consequence of the surface roughening than the increased absorption at energies approaching the surface plasma frequency. Such an interpretation also appears consistent with the results in Figure 3 showing a 3–4 times increase in the photocurrent between a mildly roughened and a deeply roughened Ag electrode. Among morphological modifications produced by the electrochemical oxidation–reduction cycles one cannot neglect the possible changes in the preferential crystallographic orientation of the roughness features. It is to be recalled, in this connection, that the plasmons in silver are expected to decay effectively (by excitation of an electron) only if propagating near the [111] direction.<sup>16</sup> This has been confirmed experimentally with plasmon-mediated photoemission being observed for orientations close to the Ag(111) face and being absent for the Ag(100) face.<sup>17,18</sup>

In addition to the changes in the maximum values of the  $\text{CO}_2$  photoreduction currents, reached at sufficiently negative potentials to be assigned entirely to the morphological changes of the silver surface, the nature of the anion present in the solution also affected the beginning of the photocurrent–potential curve. In particular, the apparent onset potential of the photocurrent in 1 M NaBr/saturated  $\text{CO}_2$  solution was shifted by ca. 0.4 V positive with respect to that recorded in 1 M  $\text{NaClO}_4$ /saturated  $\text{CO}_2$  solution. A similar shift of the onset potential was observed when the Ag electrode was first roughened in 1 M  $\text{NaClO}_4$  and

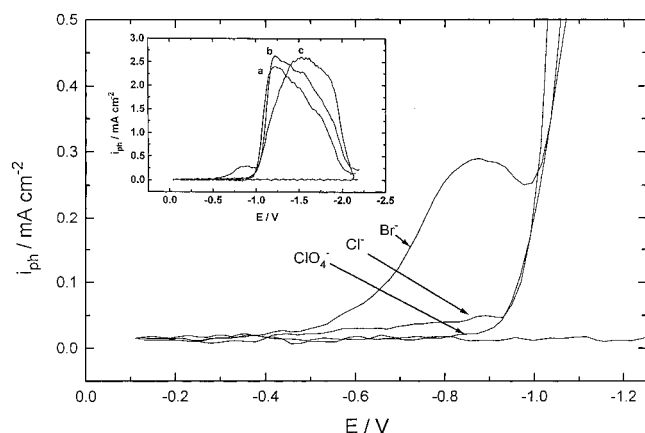
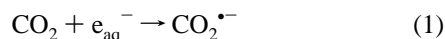


**Figure 4.** Effect of the supporting electrolyte anions on the “apparent” onset potential for the cathodic photocurrent arising from  $\text{CO}_2$  photoreduction to CO. Inset shows the same  $i_{\text{ph}}$  vs  $E$  dependence on an expanded electrode potential scale. Ag surfaces were roughened by passing  $200 \text{ mC cm}^{-2}$  of anodic charge during the silver oxidation prior to photoemission experiments in 1.0 M NaCl (a), 1.0 M NaBr (b), and 1.0 M NaClO<sub>4</sub> (c), respectively. All other experimental details as in Figure 2.

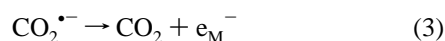
then polarized cathodically under illumination in 1M NaBr/saturated  $\text{CO}_2$  solution. Gas phase chromatographic analyses performed during the photoelectrolysis of  $\text{CO}_2$  in 1 M NaBr at a potential of  $-0.8 \text{ V}$ , located in the region of the photocurrent prewave in Figure 4, showed carbon monoxide to be the main product of  $\text{CO}_2$  reduction, in accordance with previous measurements carried out at more negative potentials.<sup>4b</sup> Both the product of  $\text{CO}_2$  reduction and the range of potentials over which this reaction occurs at the silver photocathode differ from those observed during earlier photoemission experiments performed on mercury.<sup>19</sup> In fact, in the latter case, the  $\text{CO}_2^{\bullet-}$  radical was assumed to be the primary product of solvated electron capture,



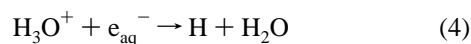
leading subsequently to the formation of formate ions:



Importantly, no photoreduction current could be recorded at the mercury cathode at potentials less negative than ca.  $-1.2 \text{ V}$  (expressed with respect to the mercuric oxide reference electrode used in the present work) due to the rapid reoxidation of  $\text{CO}_2^{\bullet-}$  anions at the electrode:



Such a behavior can be expected in view of a strongly negative equilibrium potential of the  $\text{CO}_2/\text{CO}_2^{\bullet-}$  redox couple, close to  $-2.1 \text{ V}$ .<sup>20</sup> For this reason, the involvement of  $\text{CO}_2^{\bullet-}$  anions as intermediates in the  $\text{CO}_2$  photoreduction process at silver, starting in 1 M NaBr solution already at ca.  $-0.4 \text{ V}$  (cf. Figure 4), appears unlikely. An alternative reaction pathway may be initiated by the formation in the solution of hydrogen atoms,

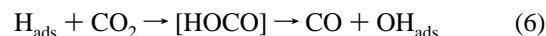


followed by their adsorption at the electrode surface:

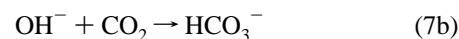


In fact, while reaction 4 is known to occur rapidly,<sup>21</sup> the recombination of hydrogen atoms in solution is a slow process as long as their concentration remains low. It has been

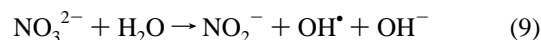
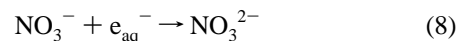
concluded on the basis of kinetic studies<sup>21</sup> that the main route of atomic hydrogen removal must involve the adsorption step (reaction 5). We postulate that  $\text{H}_{\text{ads}}$  might react with  $\text{CO}_2$  present in the solution in a way analogous to the bimolecular abstraction reaction,<sup>22</sup>



with  $\text{OH}_{\text{ads}}$  being reduced in a second electron transfer step,



The appearance of sizable photocurrents at potentials less negative than  $-0.8 \text{ V}$ , particularly pronounced in 1 M NaBr/ $\text{CO}_2$ , less marked in 1 M NaCl/ $\text{CO}_2$  (Figure 4), is to be associated with the strong adsorption underwent by halide ions at positively charged silver surface (experiments performed in a 1 M NaI/ $\text{CO}_2$  solution gave results similar to those obtained in the presence of  $\text{Br}^-$  ions). A plausible explanation of the role played in this case by the specifically adsorbed anions is the slowing down of the return of hydrated electrons to the electrode, leading normally to their reoxidation and to the drop of the photocurrent. This is supported by the fact that  $\text{Br}^-$  and  $\text{Cl}^-$  anions also affected in quite a similar way the photoreduction of nitrate ions (Figure 5). Electrochemical<sup>23</sup> as well as SERS experiments<sup>24</sup> have shown that nitrate anions are only weakly adsorbed on silver. Therefore, specifically adsorbed bromide or chloride anions are expected to replace nitrate anions on the positively charged electrode surface. Figure 6 shows that the presence of chloride or bromide anions in the solution induces a shift of the apparent onset potential for the photocurrent to  $-0.4 \text{ V}$ , as observed previously in the case of  $\text{CO}_2$  photoreduction. Photocurrents associated with the nitrate photoreduction at potentials positive to  $-1.0 \text{ V}$  are to be assigned to reactions 8–10,



representing a two-electron process, as in the case of the photoreduction of  $\text{CO}_2$  to CO. Again, the anions of the supporting electrolyte affect the magnitude of the photocurrent for the  $\text{NO}_3^-$  reduction in the order  $\text{Br}^-$ ,  $\text{Cl}^-$ ,  $\text{ClO}_4^-$ , reflecting the strength of their adsorption on silver. While bromide anions induce large photocurrents (reaching  $1 \text{ mA cm}^{-2}$ ) for the  $\text{NO}_3^-$  photoreduction in the potential range from  $-0.65$  to  $-0.9 \text{ V}$ , only residual photocurrents are observed in the presence of perchlorate anions. Further experiments demonstrated that the adsorbed  $\text{Br}^-$  and, to a lesser extent,  $\text{Cl}^-$  anions not only are able to partially block the return of hydrated electrons to the electrode but act in a similar way vs reoxidation of negatively charged reaction intermediates such as  $\text{NO}_3^{2-}$  species. It is known, in fact, that in the presence of sufficiently large concentrations of a scavenger, most of the photoemitted  $e_{\text{aq}}^-$  should be intercepted before returning back to the electrode. As shown in Figure 5b, the increase of the  $\text{NaNO}_3$  concentration in 1 M NaBr solution from 0.025 to 1 M produces a strong enhancement of the photocurrent at potentials less negative than  $-1 \text{ V}$ , due to a more effective scavenging of hydrated electrons (the maximum reached by curve b is apparently caused by the onset of a dark reduction current). A similar experiment

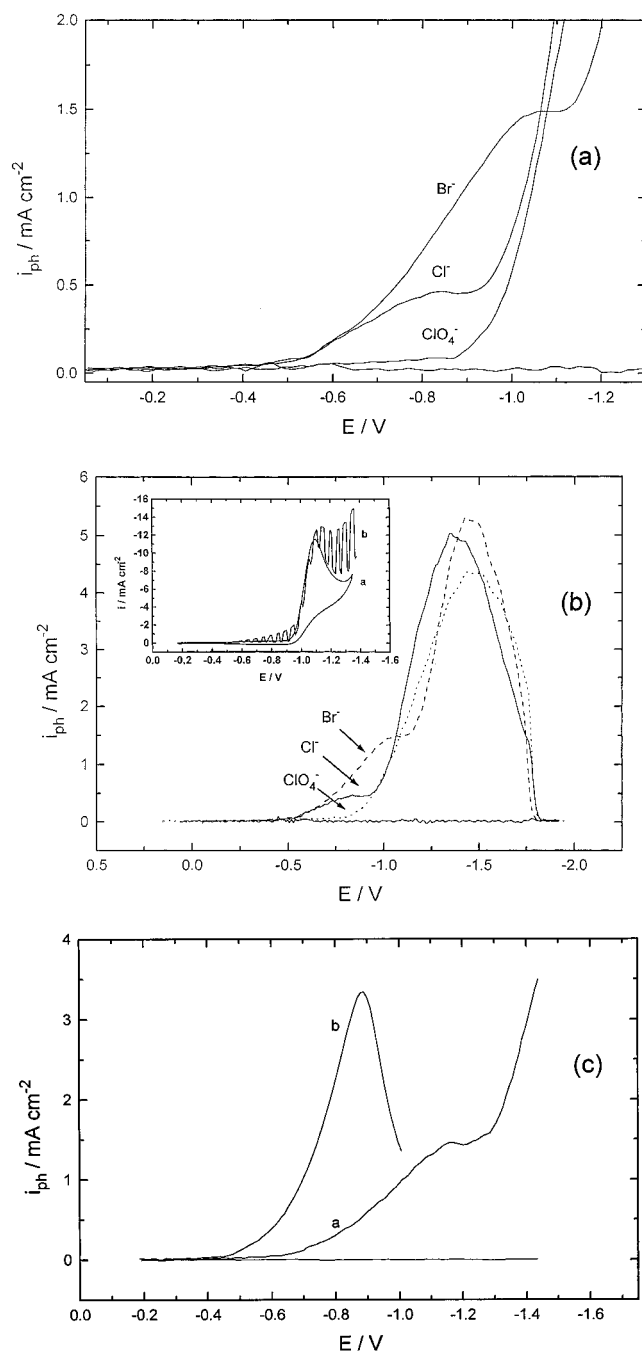


**Figure 5.** (a) "Prewave" on the photocurrent density-potential curves for the photoreduction of 25 mM nitrate (sodium salt) solution on electrochemically roughened Ag electrodes induced by the specific adsorption of anions of the supporting electrolyte on the electrode surface; 440 mW argon laser beam was chopped at a frequency  $f = 7.2$  Hz. Scan rate: 50 mV/s. (b) Curves from part a recorded on an expanded potential scale. Inset shows a dark current for the electroreduction of 25 mM nitrate, together with the superimposed cathodic photocurrent during the Ag illumination using a 440 mW argon laser beam chopped at 0.5 s intervals. Scan rate: 50 mV/s. (c) Effect of the scavenger concentration on the amount of cathodic photocurrent due to the nitrate photoreduction on Ag in the presence of 1.0 M NaBr: 25 mM NaNO<sub>3</sub> (a), 1 M NaNO<sub>3</sub> (b). Laser power: 440 mW.  $f = 7.2$  Hz. Scan rate: 50 mV/s.

performed in the presence of 1 M NaClO<sub>4</sub> revealed only very small photocurrents (more than 10 times smaller than in Figure 5b) in this potential region extending from -0.4 to -1 V. The effect of Br<sup>-</sup> ions of the supporting electrolyte was still perceptible at potentials more negative than -1 V, where they delayed the sharp increase of the photocurrent observed for both scavengers (Figures 4 and 5c). It is to be mentioned in this

connection that the latter increase of the photocurrent occurs close to the potential of zero charge, pzc, of silver (the pzc reported for Ag(110), close to that for polycrystalline silver,<sup>14a</sup> determined in 0.05 M KClO<sub>4</sub> is equal to -0.90 V<sup>25</sup>). The pzc is shifted negatively in the presence of specifically adsorbed Br<sup>-</sup> ions, more especially as their concentration in the solution is large.

A possible explanation for the unusually large amounts of the photocurrent recorded at potentials negative to -1 V may be at least a partial involvement of hot electrons reacting with the species adsorbed at the electrode surface. In such a case, the portion of Br<sup>-</sup> ions still remaining at the surface will delay the rise of the photocurrent. As shown in the inset of Figure 5c for the case of NO<sub>3</sub><sup>-</sup> ions and by earlier measurements for the case of CO<sub>2</sub>,<sup>26</sup> the sharp increase of the photocurrent at potentials more negative than -1 V coincides, in fact, with the onset of the dark reduction. In former case, the dark reaction involves from the beginning the NO<sub>3</sub><sup>-</sup> ions, which in this potential range produce nitrites. On the other hand, the initial increase of the dark current observed in the solutions containing CO<sub>2</sub> is associated with the formation of hydrogen, the reduction of CO<sub>2</sub> to give carbon monoxide starting actually at ca. -1.2 V.<sup>26</sup> Thus, in this latter case, the illumination of the Ag electrode results in a quite sensitive shift of the onset potential for the reduction of CO<sub>2</sub>, reaching 0.7 if one refers to the photocurrent "prewave" occurring in the solutions containing bromide ions.

Given the amount of the photocurrent, close to 3 mA cm<sup>-2</sup>, attained at potentials more negative than -1 V (cf. inset in Figure 4), there are no more H<sub>3</sub>O<sup>+</sup> ions but principally water molecules which are expected to serve as a source of hydrogen atoms involved in the photoreduction of CO<sub>2</sub> (reaction 6). Now, measurements performed using a rough Ag electrode immersed in various buffered solutions of the supporting electrolyte revealed only very small photocurrents, lower than 0.1 mA cm<sup>-2</sup>, associated with the hydrogen formation. This result, paralleled by the absence of any photon-driven chemistry in the case of a silver surface exposed to a water vapor,<sup>2d</sup> suggests that the illumination of the silver surface affects further stages of CO<sub>2</sub> reduction. On the other hand, the large photocurrent arising in nitrate solutions, in addition to the dark current (cf. inset in Figure 5b) is apparently due to the reduction process going beyond the 2e<sup>-</sup> stage to form ammonia.

As shown (Figure 6a) by the spectral photoresponse of the silver electrode recorded in 1 M NaBr/CO<sub>2</sub> solution, the deep roughening of the surface not only results in the strong rise of the photoyield in the range of energies corresponding to surface plasmons (with a maximum value of 5% reached at 370 nm, 3.35 eV) but also leads to a significant extension of the photoresponse toward lower energies.<sup>4c</sup> As a consequence, a sizable photoemission current is still flowing across the silver/solution interface illuminated with light of wavelengths normally used in SERS measurements and in particular with a 514.5 nm laser line (provided that the imposed electrode potential is negative enough).

Photoyield per incident photon ( $Y$ ) vs photon energy ( $h\nu$ ) data for the photoreduction of CO<sub>2</sub> in bromide and perchlorate solutions were compared using the method described by Lange et al.<sup>27</sup> Accordingly,  $Y$  vs photon energy data were integrated numerically from the threshold energy  $h\nu_{th}$  to  $h\nu$  and divided by the yield  $Y$ .

$$Y^{-1} \int Y d(h\nu) = 1/(n+1)(h\nu - h\nu_{th}) \quad (11)$$

Figure 6b shows that the dependence of  $Y$  on photon energy

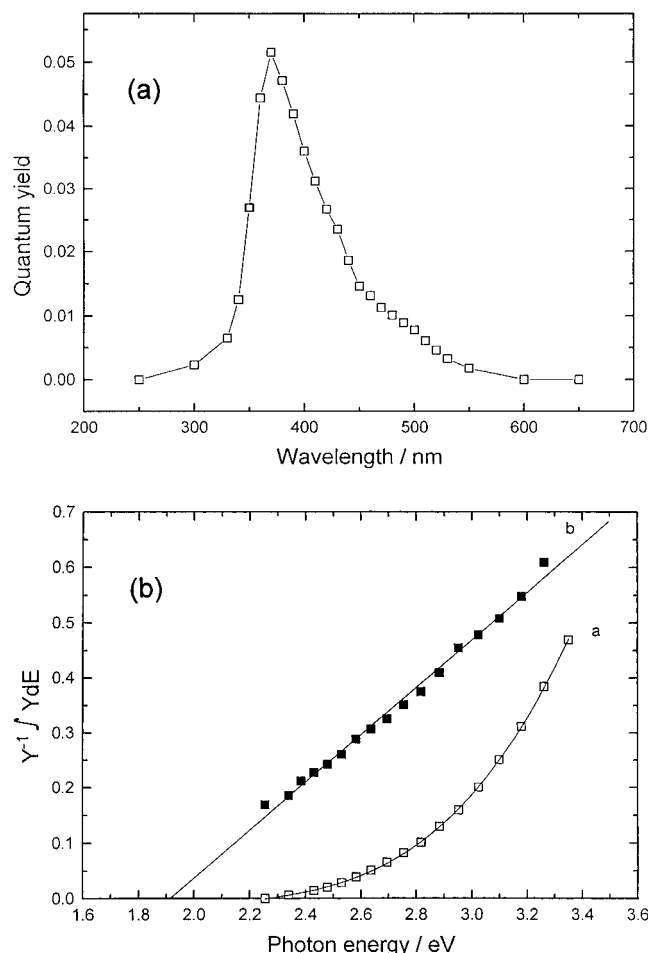


**Figure 6.** (a) Quantum yield of the photocurrent for  $\text{CO}_2$  reduction on Ag recorded at  $-1.2$  V and represented as a function of the wavelength. Sample roughened in  $1.0$  M NaBr as described in Figure 4. (b) Integrated quantum yields as a function of photon energy for  $\text{CO}_2$  photoreduction on Ag in contact with bromide (a) and perchlorate (b) solutions.

for Ag roughened in perchlorate solution is reasonably linear starting from the photon energies close to the threshold energy (about  $1.9$  eV) up to the maximum of photoyield. The value of  $n$  can be found from the slope of this line. We obtained the exponent  $n$  for the Ag electrode in perchlorate solution equal to  $1.3$ , which is significantly less than  $2.5$  (the so-called  $5/2$  law describing normally the relationship between the photoemission current and incident photon energy).<sup>28</sup> On the other hand, Lange et al.<sup>27</sup> in the case of photoemission at Cu single crystals found  $n$  values significantly higher than  $2.5$ , namely,  $3.1$ ,  $3.4$ , and  $3.7$ , for respectively (100), (110), and (111) low-index faces of Cu. Figure 6b shows also that changing the surface morphology by roughening the Ag electrode in bromide solution profoundly affects the  $Y$  vs  $h\nu$  relationship, which becomes definitely nonlinear.

## Conclusions

In many aspects the photoelectrochemical behavior of silver differs from that of other metals for which the photoemission into solution has previously been investigated. The first difference regards the effect of surface roughening, which in the case of silver not only causes a drastic enhancement of the photoyield for the wavelengths close to the surface plasmon frequency but also leads to an important extension of the photoresponse toward longer wavelengths.

The magnitude of the photocurrent arising at potentials negative with respect to the pzc (i.e. ca.  $-0.9$  V vs our reference

electrode) is controlled by rather subtle changes in surface morphology, concerning both the size and shape of surface features. Such changes may result from different chemistry involved in the oxidation/reduction of silver in the solutions of bromides, chlorides, or perchlorates as well as from increasing the extent of roughening. These changes in surface morphology affect the light absorption and, what seems even more important, the electromagnetic field density at the interface. It is just at potentials negative with respect to the pzc where a steep rise of the photocurrents related to the  $\text{CO}_2$  and/or  $\text{NO}_3^-$  reduction is observed. The specific adsorption of anions appears as a feature controlling, to a large extent, the photocathodic processes occurring at positively charged silver surface (i.e., at potentials less negative than the pzc). The actual effect of the specifically adsorbed  $\text{Br}^-$  and  $\text{Cl}^-$  ions depends on the nature of the scavenger present in the solution. In the case of photoreduction of  $\text{CO}_2$ , the presence in the solution of strongly adsorbing  $\text{Br}^-$  ions causes a significant, ca.  $0.4$  V, positive shift of the apparent onset potential. A similar positive shift of the apparent onset potential, with respect to that recorded in the solution containing weakly adsorbing  $\text{ClO}_4^-$  ions, was also observed in chloride solution. The situation is somewhat different for the photoreduction of  $\text{NO}_3^-$  ions, for which the photocurrent onset potential is already close to the equilibrium potentials of the  $\text{AgCl}/\text{Ag}/\text{Cl}^-$  and  $\text{AgBr}/\text{Ag}/\text{Br}^-$  redox couples. In the latter case, the anions of the supporting electrolyte also affect the magnitude of the photocurrent in the order  $\text{Br}^-$ ,  $\text{Cl}^-$ ,  $\text{ClO}_4^-$ , reminiscent of the strength of their adsorption on silver. While a relatively deep surface roughening is still a prerequisite to reach significant photoyields on positively charged silver surface, the addition to the solution of specifically adsorbing anions results in a further many-fold increase of the photocurrent. The fact that, under conditions of our experiments, the de Broglie wavelength of the escaping electrons should be larger than the actual thickness of the double layer makes unlikely a direct effect of the strongly adsorbed anions upon the photoemission process itself. It appears as much more probable that their role consists in slowing down the back reactions involving solvated electrons and/or intermediates returning to the electrode.

**Acknowledgment.** This work was supported by the Swiss Federal Office of Energy.

## References and Notes

- (1) (a) Pettinger, B. *Adsorption of Molecules at Metal Electrodes*; Lipkowski, J., Ross, P. N., Eds.; VCH Publishers: New York, 1992; Chapter 6. (b) Birke, R. L.; Lombardi, J. R. *Spectroelectrochemistry: Theory and Practice*; Gale, R. J., Ed.; Plenum Press: New York, 1988; Chapter 6.
- (2) (a) Nitzan, A.; Brus, L. E. *J. Chem. Phys.* **1981**, *74*, 5321. (b) Goncher, G. M.; Harris, C. B. *J. Chem. Phys.* **1982**, *77*, 3767. (c) Myli, K. B.; Grassian, V. H. *J. Phys. Chem.* **1994**, *98*, 6237. (d) Zhou, X.-L.; Zhou, X.-Y.; White, J. M. *Acc. Chem. Res.* **1990**, *23*, 327. (e) Feilchenfeld, H.; Chumanov, G.; Cotton, T. M. *J. Phys. Chem.* **1996**, *100*, 4937, and references therein.
- (3) Kim, C.-W.; Villagran, J. C.; Even, U.; Thompson, J. C. *J. Chem. Phys.* **1991**, *94*, 3974, and references therein.
- (4) (a) Kostecki, R.; Augustynski, J. *Chem. Phys. Lett.* **1992**, *194*, 386. (b) Kostecki, R.; Augustynski, J. *J. Appl. Electrochem.* **1993**, *23*, 567. (c) Kostecki, R.; Augustynski, J. *Appl. Phys.* **1995**, *77*, 4701.
- (5) Dawson, P.; Alexander, K. B.; Thompson, J. R.; Haas, J. W., III; Ferrell, T. L. *Phys. Rev. B* **1991**, *44*, 6372.
- (6) Tuschel, D. D.; Pemberton, J. E.; Cook, J. E. *Langmuir* **1986**, *2*, 380.
- (7) Sass, J. K.; Laucht, H.; Kliever, K. L. *Phys. Rev. Lett.* **1975**, *35*, 1461.
- (8) Hamelin, A.; Doubova, L.; Wagner, D.; Schirmer, H. *J. Electroanal. Chem.* **1987**, *220*, 155.
- (9) Birss, V. I.; Wright, G. A. *Electrochim. Acta* **1982**, *27*, 1429.
- (10) Birss, V. I.; Wright, G. A. *Electrochim. Acta* **1982**, *27*, 1439.
- (11) *Surface Enhanced Raman Scattering*; Chang, R. K., Furtak, T. E., Eds.; Plenum Press: New York, 1982.



- (12) Schatz, G. C. *Acc. Chem. Res.* **1984**, *17*, 370.
- (13) Bryant, M. A.; Pemberton, J. E. *Langmuir* **1990**, *6*, 751.
- (14) (a) Hamelin, A. *Modern Aspects of Electrochemistry*; Conway, B. E., White, R. E., Bockris, J. O'M., Eds.; Plenum Press: New York, 1985; No. 16, Chapter 1. (b) Kautek, W.; Gordon, J. G., II. *J. Electrochem. Soc.* **1990**, *137*, 3405. (c) Rojhtantalab, H. M.; Richmond, G. L. *J. Phys. Chem.* **1989**, *93*, 3269.
- (15) Endriz, J. G.; Spicer, W. E. *Phys. Rev. B* **1971**, *4*, 4159.
- (16) Kliewer, K. L. *Photoemission and the Electronic Properties of Surfaces*; Feuerbacher, B., Fitton, B., Willis, R. F., Eds.; Wiley Interscience: New York, 1979; Chapter 3.
- (17) Neff, H.; Sass, J. K.; Lewerenz, H. J. *Surf. Sci.* **1984**, *143*, L356.
- (18) Funtikov, A. M.; Sigalaev, S. K.; Kazarinov, V. E. *J. Electroanal. Chem.* **1987**, *228*, 197. It is to be mentioned, in this connection, that the relationship between the surface roughness and the extent of photoemission on silver has also been discussed by the above authors. However, most of their measurements were performed using a Ag(100) single crystal. On the other hand, their observed dependence of the photoemission currents on the incident light frequency did not display any maximum in the energy range corresponding normally to the plasmon excitation on silver. Therefore, it seems doubtful that the above photoeffects include any significant contribution arising from the excitation of surface plasmons.
- (19) Schiffrin, D. J. *Discuss. Faraday Soc.* **1973**, *56*, 75.
- (20) Leitner, W. *Angew. Chem., Int. Ed. Engl.* **1995**, *34*, 2207.
- (21) Pleskov, Yu. V.; Rottenberg, Z. A.; Eletsky, V. V.; Lakomov, V. I. *Discuss. Faraday Soc.* **1973**, *56*, 52.
- (22) Zewail, A. H. *J. Phys. Chem.* **1996**, *100*, 12701.
- (23) Vitanov, T.; Popov, A. *Trans. Soc. Adv. Electrochem. Sci. Technol.* **1975**, *10*, 5.
- (24) Thanos, I. C. G. *J. Electroanal. Chem.* **1986**, *200*, 231.
- (25) Hamelin, A.; Morin, S.; Richer, J.; Lipkowski, J. *J. Electroanal. Chem.* **1989**, *272*, 241.
- (26) Kostecki, R.; Augustynski, J. *Ber. Bunsen-Ges. Phys. Chem.* **1994**, *98*, 1510.
- (27) Lange, P.; Sass, J. K.; Unwin, R.; Tench, D. M. *J. Electroanal. Chem.* **1981**, *122*, 387.
- (28) Gurevich, Yu. Ya.; Pleskov, Yu. V.; Rotenberg, Z. A. *Photoelectrochemistry*; Consultants Bureau: New York, 1980.